Spatial Correlation Based Incremental Learning for Spatiotemporal Modeling of Battery Thermal Process

Bing-Chuan Wang, Han-Xiong Li, *Fellow, IEEE*, and Hai-Dong Yang

***Abstract*—The thermal effect has a significant impact on the performance of a lithium-ion (Li-ion) battery. Thus, modeling the thermal process, which always involves unknown boundary heat exchange, is significant to battery management. Two critical issues should be addressed for the thermal process modeling: 1) the nominal model which is constructed offline can be updated efficiently to compensate for any online disturbances, and 2) the influence of previous and recent spatiotemporal dynamics may be varying and should be handled properly. Bearing these in mind, a spatial correlation based incremental learning technique is designed for spatiotemporal modeling. First, the incremental learning technique is developed to update the dominant spatial basis functions (DSBFs) of the nominal model, which is constructed by a time/space separation based method. Then, a forgetting factor is incorporated into the incremental learning technique to handle time-varying dynamics. Additionally, the popular approximator, that is, the radial basis function neural network, is utilized to identify the low-dimensional temporal model. Simulations and experiments on a pouch type battery with boundary heat exchange have demonstrated the accuracy and efficiency of the proposed modeling method.**

***Index Terms*—battery thermal process, time/space separation, spatial correlation, incremental learning, forgetting factor**

I. Introduction

PURE electric vehicles (EVs), hybrid electric vehicles (HEVs), and plug-in hybrid electric vehicles have become more and more popular due to their little consumption of oil and little greenhouse emission. As the energy storage and conversion component, batteries play a significant role in EV and HEV technology. Among various kinds of batteries, Li-ion batteries have been widely adopted due to their high theoretical energy densities and tolerance to cycling [1]. The temperature effect is the main factor which limits the ability of a Li-ion battery [2], [3]. When they are charged or discharged, Li-ion batteries will generate heat which is introduced by the electrochemical reaction and Ohmic heating. On the contrary, the generated heat will affect the Li-ion batteries from various aspects such as performance, life, capacity, and safety. Thus, modeling the thermal process accurately will be beneficial to optimizing, monitoring, and controlling a battery system.

In fact, the thermal process of a Li-ion battery is a typical distributed parameter system (DPS) which is governed by partial differential equations (PDEs) [4], [5]. It is difficult to model because of its infinite-dimensional spatiotemporal nature and complex nonlinearities. The state-of-the-art models of the thermal process can be classified into two categories: 1) lumped parameter model, and 2) spatiotemporal model [6]. In the lumped parameter model, the temperature of several representative space points is estimated instead of the whole operating space [7]. In [8], the lumped thermal model is coupled with the equivalent circuit model. The lumped thermal model is also integrated with the pseudo-two-dimensional (P2D) model [9], [10]. Although the lumped parameter model can be used in a battery management system (BMS) for control purpose easily, it ignores the distributed property. Because the temperature distribution of the whole space is more preferable in many practical cases [11], [12], numerous spatiotemporal models have been proposed to approximate the temperature distribution over space [2]. Kim *et al.* [13] propose a two-dimensional PDE for the thermal process, which is solved by the finite element method (FEM). Similarly, the two-dimensional PDE is simulated by the computational fluid dynamics (CFD) method [14]. However, most numerical methods such as FEM and CFD require the exact form and parameters of the PDE to be known. Additionally, they are time-consuming. Thus, various reduced-order models are proposed [15]. The spectral method reduces the PDEs describing the electrochemical-thermal behavior of Li-ion battery stacks into several ordinary differential equations (ODEs) [16]. In this study, the spatial domains of the positive electrode, the separator, and the negative electrode are transformed into a normalized domain. Then, the cosine functions and the orthogonal collocation are used as the DSBFs and the model reduction method, respectively. Similarly, the orthogonal collocation and the Chebyshev polynomials are designed to simplify the pseudo-three-dimensional model [17], as well as the stochastic spectral projection and the orthogonal Hermite polynomials for the electrochemical-thermal model [18]. However, the spectral method can only work for the parabolic DPSs with homogeneous boundary conditions, under the assumption that the preliminary knowledge is known.

Karhunen-Loève (KL) method [19] is another representative method which has been extensively applied to model the

This work was supported in part by the General Research Fund Project from Research Grant Council of Hong Kong SAR (CityU: 11205615), and in part by the National Natural Science Foundations of China under Grant U1501248. (*Corresponding author*: Han-Xiong Li.)

B.-C. Wang is with the Department of Systems Engineering and Engineering Management, City University of Hong Kong, and also with the State Key Laboratory of High Performance Complex Manufacturing, Central South University, Changsha, China (e-mail: wangbingchuancityu@gmail.com).

H.-X. Li is with the Department of Systems Engineering and Engineering Management, City University of Hong Kong (e-mail: mehxli@cityu.edu.hk).

H.-D. Yang is with Guangdong Engineering Research Center for Green Manufacturing & Energy Efficiency Optimization, Guangdong University of Technology, Guangzhou, China (e-mail: yanghd@yeah.net).

thermal process of a Li-ion battery. KL is utilized to simplify the electrochemical-thermal model of a Li-ion battery [20]. The reduced-order model agrees well with the COMSOL model [21]. KL is also utilized to model the thermal process of a one-dimensional battery. In order to compensate for the model-plant mismatch caused by the spatial nonlinearity and other uncertainties, a data-based neural model is presented [3]. This method is extended to model a two-dimensional thermal process, where the extreme learning machine (ELM) is utilized to construct the temporal model [22].

As described above, most KL based methods focus on constructing an offline model, while little effort has been devoted to online modeling. When KL is applied to construct an online model, the efficiency must be considered. Recently, an incremental KL modeling is designed to improve the efficiency of online DPS modeling [23]. By utilizing the incremental technique, the incremental KL can avoid the repeated eigenvalue decomposition of the temporal correlation matrix, and thus significantly reduce the computational cost. As a result, its efficiency can be promoted. However, it treats all acquired data equally that may not be effective in many situations. For example, when a Li-ion battery is working under unknown boundary heat exchange [24], [25], the boundary conditions are time-dependent. For these processes, the out-of-date data cannot reflect the real-time spatiotemporal dynamics. Thus, methods considering all data equally will lose their effectiveness to some extent. There is an urgent need in real applications to design an effective method for the online spatiotemporal modeling of a Li-ion battery under unknown boundary heat exchange.

Recently, a sliding window based KL (SW-KL) is proposed to model DPSs with time-dependent boundary conditions [26], where a sliding window is utilized to capture the recent spatiotemporal dynamics. A forgetting factor is also introduced to adjust the influence of previous and recent data. Experiment comparisons demonstrate the superior performance of SW-KL and its potential in industrial applications. However, the computational complexity of SW-KL highly depends on the number of sensors utilized for data collection. As the higher accuracy is required, the more sensors will be needed that will cause the higher computational complexity. The method should be further upgraded to reduce the computational complexity, while maintaining the required modeling accuracy.

Based on these observations, an upgraded incremental KL is proposed to model the thermal process with time-dependent boundary conditions in a Li-ion battery. When constructing an analytical model of the considered process, we should address two issues: 1) the DSBFs can be updated efficiently, and 2) the influence of previous and recent data can be adjusted effectively. To address the first issue, the incremental technique is utilized to update the DSBFs recursively instead of calculating them from scratch. Different from the temporal correlation based incremental KL (t-incremental KL) [23], a spatial correlation based incremental KL is proposed, where a forgetting factor can be attached more easily. By tuning the forgetting factor, the influence of previous and recent data can be adjusted effectively. Due to its numerous advantages, such as super approximation ability and ease of implementation, the radial basis function neural network (RBFNN) [27] is employed to develop the temporal model. The contributions of this paper are summarized as follows:

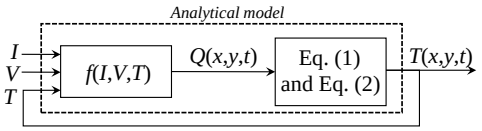

Fig. 1. Modeling of temperature distribution in a battery.

- A spatial correlation based incremental KL is proposed.
- By using a forgetting factor, the proposed method can balance the spatiotemporal dynamics at different instants effectively.
- Simulations and experiments on a single battery cell and a composite cell under unknown boundary heat exchange validate the advantages of the proposed method.

The rest of the paper is organized as follows: the considered thermal process is described in Section II; The proposed method is detailed in Section III; Section IV includes the simulation studies and discussions; The experiment details are given in Section V, and Section VI summarizes the concluding remarks.

II. Problem Description

The thickness of the battery cell is much shorter than that of other dimensions. The temperature variation along this direction could be neglected. Additionally, it is nearly impossible to place a sensor along this direction. Thus, the two-dimensional thermal process of a Li-ion battery, which is utilized widely [13], [22], [28], is considered:

$$\rho C_p \frac{\partial T}{\partial t} = \frac{\partial}{\partial x}(\lambda_x \frac{\partial T}{\partial x}) + \frac{\partial}{\partial y}(\lambda_y \frac{\partial T}{\partial y}) + Q(x,y,t), \quad (1)$$

involving boundary condition:

$$-\lambda_x \frac{\partial T}{\partial x} - \lambda_y \frac{\partial T}{\partial y} = h(T - T_{air}), \quad (2)$$

where $T(x,y,t)$ is the time/space coupled temperature; x and y are the spatial coordinates; t is the time variable; ρ is the battery density; C_p is the cell heat capacity; λ_x and λ_y are the thermal conductivities across x and y directions, respectively; T_{air} is the environment temperature, and h denotes the convective coefficient. Note that h is time-varying due to the unknown boundary heat exchange. Thus, the boundary condition is time-dependent. $Q(x,y,t)$ is the heat generation term. As shown in [13], [22], it is described as follows:

$$Q = aJ[E_{oc} - (V_p - V_n) - T\frac{\mathrm{d}E_{oc}}{\mathrm{d}T}] + a_p r_p i_p^2 + a_n r_n i_n^2, \quad (3)$$

where a is the specific area of the battery; J is the current density; E_{oc} is the open-circuit potential; $V = V_p - V_n$ is the cell voltage; a_p and a_n are the specific area of the positive and negative electrodes, respectively; i_p and i_n denote the linear current density; r_p and r_n are the resistances. As can be seen, $Q(x,y,t)$ is a nonlinear function of the lumped current I, voltage V, and T, that is, $Q(x,y,t) = f(I,V,T)$ [25]. By combining $Q(x,y,t) = f(I,V,T)$ with Eqs. (1) and (2), the

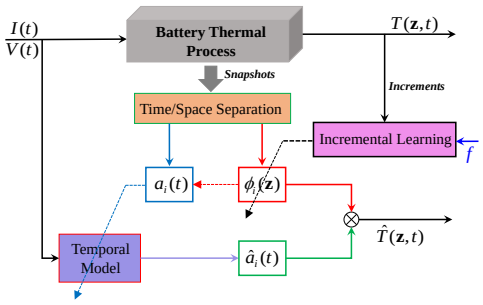

Fig. 2. Framework of the proposed modeling method.

relationship between (I, V) and T can be described as shown in Fig. 1. As shown in the figure, $Q(x, y, t)$ is an intermediate variable that connects (I, V) with T. That is to say, T can be considered as generated by I and V. Note that this paper aims to propose a data-driven model. In addition, it is hard to measure $Q(x, y, t)$ accurately in real applications. Thus, an analytical model can be constructed by mapping (I, V) to T directly. If the model of $Q(x, y, t) = f(I, V, T)$ is known, it can be integrated to enhance the modeling performance.

III. Spatial Correlation Based Incremental Spatiotemporal Modeling

A. Framework

As shown in Fig. 2, the proposed modeling method is time/space separation based. To be specific, the data-driven method KL is utilized to separate the thermal process into n nominal DSBFs $\{\phi_i(\mathbf{z})\}_{i=1}^n$ and temporal coefficients $\{a_i(t)\}_{i=1}^n$. Note that the spatial vector $\mathbf{z}$ is equal to (x, y). When new data/a set of increments is coming, an incremental learning technique, that is, spatial correlation based incremental KL is developed to update the previous DSBFs. By a forgetting factor f, the influence of the previous DSBFs can be adjusted. Afterward, the new DSBFs are combined with the increments to tune the temporal coefficients. Then, the temporal model, which is utilized for prediction, is updated by the new temporal coefficients. Finally, by time/space synthesis, the time/space coupled temperature can be predicted.

The main elements of the proposed method will be described in detail. First, the spatial correlation based incremental KL is presented. Next, the forgetting factor is introduced. Finally, the RBFNN based temporal model is elaborated.

B. Spatial Correlation Based Incremental KL

In the conventional KL [19], in order to construct the nominal model, L snapshots $\mathbf{T} \in \Re^{N\times L}$ are sampled as measurements by N sensors. The spatial correlation matrix of these snapshots can be calculated as follows:

$$\bar{R} = \frac{1}{L}\mathbf{T}\mathbf{T}^\top. \tag{4}$$

Afterward, we can obtain the DSBFs by decomposing $\bar{R}$ with eigenvalue decomposition:

$$\bar{R} = U\Delta U^\top, \tag{5}$$

where U is an orthogonal matrix and Δ is a diagonal matrix. Subsequently, the n columns of U corresponding to the first n largest eigenvalues are selected as the DSBFs, those are, $\bar{\phi}_1(\mathbf{z}), \bar{\phi}_2(\mathbf{z}), \cdots, \bar{\phi}_n(\mathbf{z})$. The matrix U can also be calculated by decomposing $\mathbf{T}$ with singular value decomposition (SVD):

$$\mathbf{T} = U\Sigma V^\top, \tag{6}$$

where U and V are two orthogonal matrices, and Σ is a diagonal matrix. Additionally, the rank-n approximation of $\mathbf{T}$ is described as follows:

$$\mathbf{T} \approx U_n\Sigma_n V_n^\top, \tag{7}$$

where U_n, Σ_n, and V_n are the rank-n approximation of U, Σ, and V, respectively. Σ_n is a diagonal matrix whose diagonal values are the first n largest ones among those of Σ. Note that each column of U_n represents a discrete DSBF.

When l new snapshots $\mathbf{D} \in \Re^{N\times l}$ come, the expanded matrix $[\mathbf{T}\ \mathbf{D}]$ can be obtained. In the conventional KL, SVD of $[\mathbf{T}\ \mathbf{D}]$ is utilized to update the DSBFs, which would be extremely time-consuming. To avoid repeatedly executing SVD on the expanded matrix, $[\mathbf{T}\ \mathbf{D}]$ is reformulated as follows:

$$\begin{bmatrix} \mathbf{T} & \mathbf{D} \end{bmatrix} \approx \begin{bmatrix} U_n & Q \end{bmatrix} \begin{bmatrix} \Sigma_n & U_n^\top\mathbf{D} \\ 0 & R \end{bmatrix} \begin{bmatrix} V_n^\top & 0 \\ 0 & I_l \end{bmatrix}, \tag{8}$$

where $I_l \in \Re^{l\times l}$ is an identity matrix; Q is an orthogonal matrix; R is an upper triangular matrix; Q and R can be derived by the QR decomposition:

$$QR = (I_N - U_nU_n^\top)\mathbf{D}, \tag{9}$$

where $I_N \in \Re^{N\times N}$ is an identity matrix; $Q \in \Re^{N\times m}$ and $R \in \Re^{m\times l}$; $m = \min\{N, l\}$ is the rank of $(I_N - U_nU_n^\top)\mathbf{D}$. Next, we can decompose $\begin{bmatrix} \Sigma_n & U_n^\top\mathbf{D} \\ 0 & R \end{bmatrix}$ by SVD:

$$\begin{bmatrix} \Sigma_n & U_n^\top\mathbf{D} \\ 0 & R \end{bmatrix} = \tilde{U}\tilde{\Sigma}\tilde{V}^\top, \tag{10}$$

where $\tilde{U}$ and $\tilde{V}$ are orthogonal matrices; $\tilde{\Sigma}$ is a diagonal matrix. By combining Eq. (8) with Eq. (10), we can derive:

$$\begin{bmatrix} \mathbf{T} & \mathbf{D} \end{bmatrix} \approx \left(\begin{bmatrix} U_n & Q \end{bmatrix}\tilde{U}\right)\tilde{\Sigma}\left(\begin{bmatrix} V_n & 0 \\ 0 & I \end{bmatrix}\tilde{V}\right)^\top. \tag{11}$$

It can easily be known that $\begin{bmatrix} U_n & Q \end{bmatrix}$ is an orthogonal matrix. Consequently, $\left(\begin{bmatrix} U_n & Q \end{bmatrix}\tilde{U}\right)$ is an orthogonal matrix. Similarly, $\left(\begin{bmatrix} V_n & 0 \\ 0 & I \end{bmatrix}\tilde{V}\right)^\top$ is an orthogonal matrix. As a result, Eq. (11) can approximate the SVD of $\begin{bmatrix} \mathbf{T} & \mathbf{D} \end{bmatrix}$. Thus, the n columns of $\left(\begin{bmatrix} U_n & Q \end{bmatrix}\tilde{U}\right)$ corresponding to the first n largest singular values can be regarded as the new DSBFs. In this manner, the efficiency can be improved.

Computational complexity analysis: Based on the above derivations, the two key steps of the spatial correlation based incremental KL are: 1) QR decomposition of $(I_N - U_nU_n^\top)\mathbf{D} \in \Re^{N\times l}$, and 2) SVD of $\begin{bmatrix} \Sigma_n & U_n^\top\mathbf{D} \\ 0 & R \end{bmatrix} \in \Re^{(n+m)\times(n+l)}$. The QR decomposition requires approximately $O(Nl^2)$ flops and the SVD needs approximately $O((n+l)(n+$

$m)^2$) flops. In real applications, the number of DSBFs (i.e., n) is very small, that is, $n \ll \{L, N, l, m\}$. Consequently, $O((n+l)(n+m)^2)$ is approximately equal to $O(lm^2)$. Because $m = \min\{N, l\}$, $lm^2 < Nl^2$. In summary, the computational complexity of the proposed method is $O(Nl^2)$. In the conventional KL, we should conduct SVD on $\begin{bmatrix} \mathbf{T} & \mathbf{D} \end{bmatrix} \in \Re^{N\times(L+l)}$, which needs approximately $O((L+l)N^2)$ flops. As we know, L increases as time progresses. In many cases, l is less than N. Thus, we can conclude that the proposed method is more efficient than the conventional KL. In SW-KL, we should conduct eigenvalue decomposition on the new correlation matrix, which needs approximately $O(N^3)$ flops. As can be seen, the computational efficiency of the proposed method is less dependent on N. If many sensors are needed for high accuracy, the proposed method would be more proper than SW-KL.

C. Forgetting Factor

When a DPS with time-dependent boundary conditions is modeled, it is likely that recent data will be more indicative than the previous data. However, as time progresses, the previous data can be very large, which will render the model blind to changes in the data stream. To address this issue, the contribution of previous data should be down-weighted. In the conventional KL, the eigenfunctions with big eigenvalues will be selected as the DSBFs. Since the eigenvalues and eigenfunctions are calculated from the spatial correlation matrix, this matrix has a significant impact on the DSBFs. A forgetting factor f ($0 \le f \le 1$) can be attached to the spatial correlation matrix of previous data to reduce its impact [26].

In the proposed method, SVD of $\begin{bmatrix} \Sigma_n & U_n^\top \mathbf{D} \\ 0 & R \end{bmatrix}$ is conducted instead of conducting the eigenvalue decomposition on the spatial correlation matrix of all data. According to Eqs. (4)-(6), we can find that $\Sigma^2 = L\Delta$, where Δ is the eigenvalue matrix of the spatial correlation matrix. Thus, the forgetting factor can be attached to Σ_n to reduce the impact of previous data. In this case, we can conclude that the contribution of previous data to the overall correlation matrix would be reduced by an additional coefficient f^2. The proof is given as follows. Because $[U_n \ Q]$ is an orthogonal matrix, the singular values of $(\begin{bmatrix} U_n & Q \end{bmatrix} \begin{bmatrix} f\Sigma_n & U_n^\top \mathbf{D} \\ 0 & R \end{bmatrix})$ are the same as those of $\begin{bmatrix} f\Sigma_n & U_n^\top \mathbf{D} \\ 0 & R \end{bmatrix}$. Furthermore, calculating the left-singular functions and singular values of $(\begin{bmatrix} U_n & Q \end{bmatrix} \begin{bmatrix} f\Sigma_n & U_n^\top \mathbf{D} \\ 0 & R \end{bmatrix})$ is equal to calculating the eigenfunctions and the square roots of the eigenvalues of $(\begin{bmatrix} U_n & Q \end{bmatrix} \begin{bmatrix} f\Sigma_n & U_n^\top \mathbf{D} \\ 0 & R \end{bmatrix})(\begin{bmatrix} U_n & Q \end{bmatrix} \begin{bmatrix} f\Sigma_n & U_n^\top \mathbf{D} \\ 0 & R \end{bmatrix})^\top$. Further expanding this equation, we can get that: $\begin{bmatrix} fU_n\Sigma_n & \mathbf{D} \end{bmatrix} \begin{bmatrix} f\Sigma_n^\top U_n^\top \\ \mathbf{D}^\top \end{bmatrix} = f^2 U_n\Sigma_n\Sigma_n {U_n}^\top + \mathbf{D}\mathbf{D}^\top \approx f^2\mathbf{T}\mathbf{T}^\top + \mathbf{D}\mathbf{D}^\top$. As a result, the contribution of previous data is reduced by a coefficient f^2.

The forgetting factor f would have an impact on the proposed method. Similar to [26], the selection process is formulated as an optimization problem. Different from [26], the leave-one-out cross-validation is used to increase accuracy. Additionally, an outstanding evolutionary algorithm called CoDE [29] is used to generate new solutions. The main steps are given as follows:

Step 1: Initialize a population of f^2 as parents.

Step 2: Utilize CoDE to generate new offsprings.

Step 3: Utilize leave-one-out cross-validation to evaluate each offspring.

Step 4: Select the best one among each parent and its offsprings.

Step 5: If the stopping criterion is satisfied, then stop the procedure, otherwise, go to step 2.

D. Main Advantages of the Spatial Correlation Based Incremental KL

- The proposed method is more efficient and can capture the recent spatiotemporal dynamics more effectively than the conventional KL.
- The proposed method can capture the recent spatiotemporal dynamics more effectively than t-incremental KL.
- The proposed method would be more efficient than SW-KL if lots of sensors are needed for high accuracy.
- The proposed method is more efficient than the FEM and more accurate than the spectral method.
- The proposed method does not require the PDE which describes the thermal process to be known.

In summary, the proposed method can achieve better accuracy and efficiency. Some remarks are summarized as follows:

Remark 1: As shown in [30] and [31], the thermal process of a composite cell and that of a battery pack can both be described as parabolic DPSs. Since the proposed method is based on KL [19], it would be effective to model parabolic DPSs not limited to a two-dimensional system. Thus, if some temperature data in a battery pack can be measured, the proposed method could be used directly. Otherwise, similar to [32], the model can be decoupled into two submodels. To model the temperature distribution of the composite cell containing several cells, the proposed method can be used, which has been validated by simulations and experiments in the supplementary file. The temperature variation across the entire pack can be estimated by a lumped parameter model. Note that the data for modeling the composite cell can be acquired mathematically as shown in the following remarks.

Remark 2: The proposed method is based on a data-driven method, that is, KL. Thus, some sensors are needed to acquire data. The proposed method is to provide performance prediction for a battery with unknown boundary heat exchange, which would be difficult for conventional methods. The only limitation for its application is that a number of sensors are used. In our future study, we would be devoted to estimating the time-varying convective coefficient online. As a result, data can be acquired mathematically. Without the utilization of real sensors, the proposed method could be added to a BMS more easily.

Remark 3: To estimate the parameters of a battery, an electrochemical thermal model can be first constructed mathematically [33], [34]. Since the temperature would have a

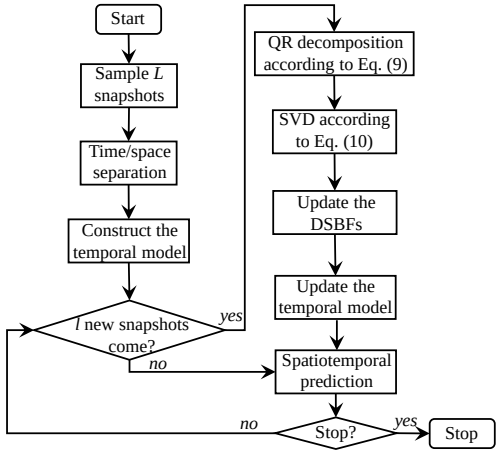

Fig. 3. Flowchart of the proposed modeling method.

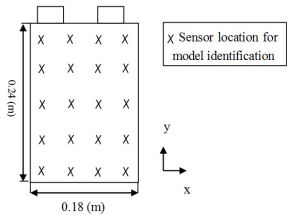

Fig. 4. Sensor location for sampling data.

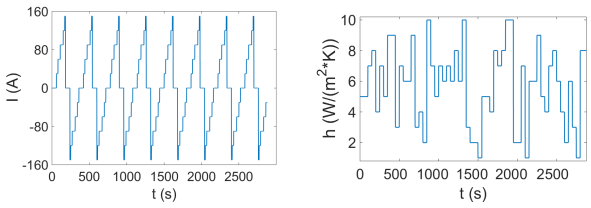

(a) (b)

Fig. 5. Input current and h for modeling: (a) Input current, (b) h.

critical impact on the electrochemical properties, the error between the output voltage of the model and that of the battery can be used to evaluate the thermal parameters. By using a direct search method to minimize the error, we can estimate the parameters. To further improve the efficiency of optimization, both the surrogate model [35] and transfer optimization [36] can be used. Note that the proposed model and the parameter estimation process would be executed in a parallel manner.

E. Dynamic Modeling of Temporal Coefficients

As shown in Fig. 2, once the temporal coefficients $\mathbf{a}(t) = \{\mathbf{a}_1, \cdots, \mathbf{a}_n\}$ are obtained as

$$\mathbf{a}_i = \bar{\phi}_i^\top \begin{bmatrix} \mathbf{T} & \mathbf{D} \end{bmatrix}, i = 1 \cdots n, \tag{12}$$

a temporal model needs to be constructed for prediction, where $\mathbf{a}_i$ is the discrete form of $a_i(t)$. Taking the input signal $\mathbf{u}(t) = \{\boldsymbol{u}_1, \cdots, \boldsymbol{u}_m\}$ into consideration, we can formulate the temporal model mathematically as follows:

$$\mathbf{a}(t) = F(\mathbf{a}(t-1), \cdots, \mathbf{a}(t-n_a), \mathbf{u}(t-1), \cdots, \mathbf{u}(t-n_b)) + \varepsilon(t), \tag{13}$$

where n_a and n_b are the maximum output and input lags, respectively; $F(\cdot)$ is a nonlinear function used to capture the temporal dynamics, and $\varepsilon(t)$ is the residual error. Various machine learning techniques, such as ELM [22] and Bayesian neural network [37], can be utilized to learn $F(\cdot)$.

RBFNN is a kind of interpolation model. It owns numerous merits including ease of implementation and universal approximation ability [27]. Thus, it is adopted to construct the temporal model:

Step 1: Specify the input and output at time instant t as $\boldsymbol{\alpha}(t) = [\mathbf{a}_1(t-n_a : t-1), \cdots, \mathbf{a}_n(t-n_a : t-1), \mathbf{u}_1(t-n_b : t-1), \cdots, \mathbf{u}_m(t-n_b : t-1)]$ and $\boldsymbol{\Gamma}(t) = [\mathbf{a}_1(t), \cdots, \mathbf{a}_n(t)]$, respectively.

Step 2: Set $n_a = 1$, $n_b = 1$, and $L = L + l$. Then, arrange the temporal coefficients derived from L snapshots as training inputs and outputs:

$$\boldsymbol{\Psi} = \begin{bmatrix} K(\boldsymbol{\alpha}(2), \boldsymbol{\alpha}(2)) & \cdots & K(\boldsymbol{\alpha}(2), \boldsymbol{\alpha}(L)) \\ \vdots & \ddots & \vdots \\ K(\boldsymbol{\alpha}(L), \boldsymbol{\alpha}(2)) & \cdots & K(\boldsymbol{\alpha}(L), \boldsymbol{\alpha}(L)) \end{bmatrix}, \widetilde{\boldsymbol{\Gamma}} = \begin{bmatrix} \boldsymbol{\Gamma}(2) \\ \vdots \\ \boldsymbol{\Gamma}(L) \end{bmatrix}$$

Step 3: Map inputs to outputs by RBFNN as $\widetilde{\boldsymbol{\Gamma}} = \boldsymbol{\Psi}\mathbf{W}$, with

$$\mathbf{W} = \begin{bmatrix} w_{1,1} & \cdots & w_{1,n} \\ \vdots & \ddots & \vdots \\ w_{L-1,1} & \cdots & w_{L-1,n} \end{bmatrix}.$$

Step 4: Calculate the weight matrix $\mathbf{W}$ as: $\mathbf{W} = (\boldsymbol{\Psi}^\top \boldsymbol{\Psi})^{-1} \boldsymbol{\Psi}^\top \widetilde{\boldsymbol{\Gamma}}$.

Step 5: Consequently, the temporal coefficients at time instant $t (t > L)$, that is, $\hat{\mathbf{A}}_t$, can be predicted as follows:

$$\begin{bmatrix} \hat{\mathbf{a}}_1(t) \\ \vdots \\ \hat{\mathbf{a}}_n(t) \end{bmatrix} = \mathbf{W}^\top \begin{bmatrix} K(\boldsymbol{\alpha}(t), \boldsymbol{\alpha}(2)) \\ \vdots \\ K(\boldsymbol{\alpha}(t), \boldsymbol{\alpha}(L)) \end{bmatrix}.$$

$K(\boldsymbol{\eta}, \boldsymbol{\eta}') = e^{-\gamma \|\boldsymbol{\eta} - \boldsymbol{\eta}'\|_2^2}$ is the Gaussian radial basis function (RBF) with γ the spread parameter. $w_{i,j}$ is the weight between the ith hidden neuron and the jth output neuron. Finally, the temperature distribution over space can be achieved by spatiotemporal synthesis: $\hat{\mathbf{T}}_t = [\bar{\phi}_1, \cdots, \bar{\phi}_n]\hat{\mathbf{A}}_t$. Note that the RBF $K(\cdot)$ in an RBFNN is different from the DSBF $\bar{\phi}_i$. The former is a user-defined kernel function and is used to capture nonlinear dynamics of time series, while the latter is extracted from a DPS and is used for spatiotemporal modeling.

In summary, the whole process of the proposed modeling method is described in Fig. 3.

IV. Simulation Studies and Discussions

A. Simulation Setup

In this section, an electrochemical-thermal model, where the P2D model and the two-dimensional thermal model described in Eq. (1) are coupled, is constructed by a commercial software package COMSOL. In the model, the electrode materials are LiFePO4 and graphite. Afterward, it is used to validate the advantages of the proposed modeling method. The geometry of the battery is described in Fig. 4. As shown in the figure, 20 probes (i.e., sensors) are allocated uniformly on the surface of

TABLE I
PARAMETER SETTING OF THE PROPOSED MODELING METHOD

Parameter	l	f	n	n_a	n_b
Value	5	$\sqrt{0.3}$	5	1	1

TABLE II
THE TOTAL $RMSE$S AND CONSUMED TIME OF THE SIMULATION

Method	conventional KL	SW-KL	t-incremental KL	proposed method
$RMSE$	1.5809	**0.0875**	1.6319	**0.0875**
Total time (s)	3209.63	57.47	3309.69	**44.80**

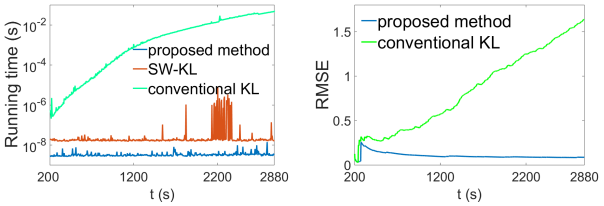

(a) (b)

Fig. 6. Performance comparison: (a) Running time, (b) online $RMSE$.

the battery for data sampling. To compare different methods, the root of mean square error ($RMSE$) is adopted:

$$RMSE = \sqrt{\frac{1}{NL}\sum_{i=1}^{N}\sum_{j=1}^{L}(T(\mathbf{z}_i,t_j)-\hat{T}(\mathbf{z}_i,t_j))^2}, \quad (14)$$

where $T(\mathbf{z}_i,t_j)$ and $\hat{T}(\mathbf{z}_i,t_j)$ are the measured and estimated temperature, respectively.

Conventionally, to excite the thermal process adequately, an appropriate input signal should be utilized. Similar to [5], a multi-step input current, which is described in Fig. 5 (a), is used. Similar to [25], h is set to a time-varying value to simulate the unknown boundary heat exchange, which is described in Fig. 5 (b). A set of 2880 snapshots is sampled for online modeling where the sampling interval is 1s. The main parameters are given in Table I. The modeling accuracy and efficiency are compared with those of the conventional KL, t-incremental KL, and SW-KL. The parameter settings of the three methods are the same as the original papers. For fair comparison, all modeling methods use RBFNN for temporal model construction, and n is the same in four methods.

B. Comparisons and Discussions

For all methods, the first 200 snapshots are employed to construct the nominal model, while the rest 2680 ones are utilized for online prediction. The simulation studies are performed on a computer with Intel Core (TM) i7-3770 (3.40 GHz) processor, 32 GB RAM, and Windows10 (64 bit) system. The total $RMSE$s and consumed time are summarized in Table II. As shown in the table, compared with the conventional KL and t-incremental KL, which consume much time to construct the temporal model, the proposed modeling method can obtain better $RMSE$ with less time. It seems that SW-KL can achieve the similar accuracy. In fact, the proposed method can improve the efficiency of SW-KL by 22%, which could be considered as a significant improvement. The time for obtaining the DSBFs is described in Fig. 6 (a). The result shows that the proposed method is more efficient than the other two methods consistently. Furthermore, the results of the conventional KL and the proposed method in terms of online $RMSE$ are shown in Fig. 6 (b), which demonstrate that the proposed method is better than the conventional KL consistently. Since the main advantage of the proposed method over SW-KL is the low computational complexity, the $RMSE$ of SW-KL is not shown in Fig. 6 (b). In summary, the proposed modeling method is accurate and efficient.

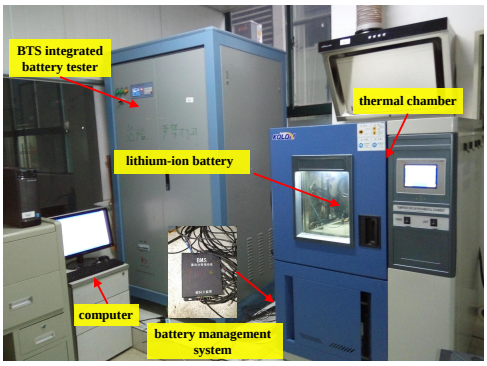

Fig. 7. Experiment platform.

V. EXPERIMENT VALIDATION

A. Experiment Setup

To further validate the advantages of the proposed method, some data is sampled from a real experiment where a pouch type Li-ion battery with LiFePO4/graphite is used. The thickness, length, and width of the battery are 7.83E-3m, 0.24m, and 0.18m, respectively. The nominal capacity, nominal voltage, charge cut-off voltage, and discharge cut-off voltage are 60Ah, 3.2V, 3.65V, and 2V, respectively. A platform composed of a battery thermal system (BTS) integrated battery tester, a thermal chamber, a BMS module, and a computer as shown in Fig. 7 is utilized to charge and discharge the battery. The same current described in Fig. 5 (a) is generated in the experiment. The BTS integrated battery tester is used to generate charge/discharge current. In the thermal chamber, a steady ambient temperature 25 °C can be guaranteed. As shown in Fig. 4, 20 sensors are allocated uniformly on the surface of the battery. Additionally, the BMS module is used to collect the temperature data. In the experiment, a host computer is used to integrate these devices together. Note that a forced-air convective cooling is employed as the unknown boundary heat exchange. Indeed, h can be identified or estimated. However, in the proposed method, the exact value of h is not needed. As the same as Section IV, a set of 2880 snapshots is sampled for online modeling.

B. Experiment Results

The 2880 snapshots are utilized to evaluate the performance of the proposed method. Similarly, the first 200 snapshots are utilized to construct the nominal model, while the rest 2680 ones are used for online performance evaluation. First, we compare the performance of the proposed method with

TABLE III
THE TOTAL $RMSE$S AND CONSUMED TIME OF THE EXPERIMENT

Method	conventional KL	SW-KL	t-incremental KL	proposed method
$RMSE$	0.8312	0.0451	1.1149	**0.0444**
Total time (s)	3064.2469	53.55	3104.46	**42.18**

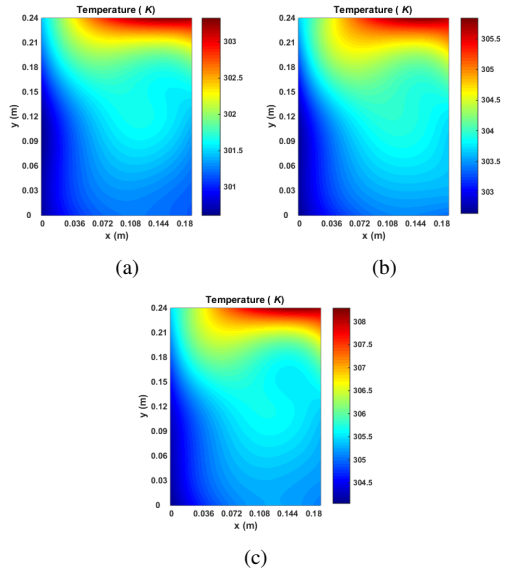

(a) (b) (c)

Fig. 8. Measured temperature distribution: (a) 960s, (b) 1920s, (c) 2880s.

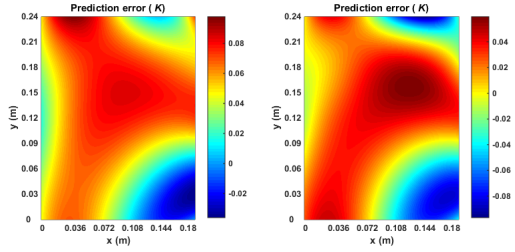

(a) (b)

Fig. 9. Prediction error at 960s: (a) conventional KL, (b) proposed method.

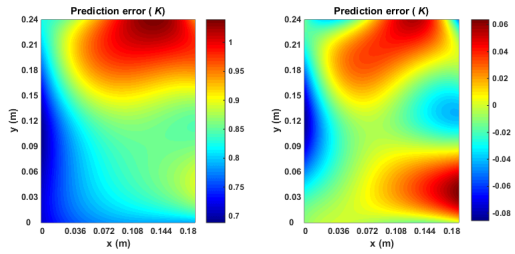

(a) (b)

Fig. 10. Prediction error at 1920s: (a) conventional KL, (b) proposed method.

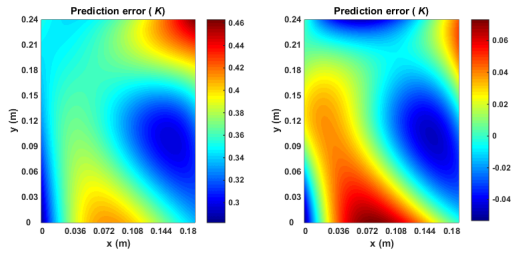

(a) (b)

Fig. 11. Prediction error at 2880s: (a) conventional KL, (b) proposed method.

that of the conventional KL, t-incremental KL, and SW-KL according to the $RMSE$ and consumed time. As shown in Table III, the proposed method performs better than the other three methods. Specifically, the efficiency of SW-KL can be improved by 21%, which could be considered as a significant improvement.

To further analyze the advantages of the proposed method, we compare the distributed prediction error of the proposed method with that of the conventional KL. The measured temperature distributions at 960s, 1920s, and 2880s are described in Fig. 8. The prediction errors are described in Figs. 9, 10, and 11. As shown in Fig. 9, the advantages of the proposed method over the conventional KL is not significant. That is to say, when the size of the data set is not big, the conventional KL can capture the spatiotemporal dynamics. However, when time progresses, the performance of the conventional KL would become worse and worse. The reason is that it cannot capture the recent spatiotemporal dynamics. On the contrary, the proposed method can achieve it successfully. The experiment results are in line with the analyses in Section III. In summary, the proposed method is effective to model the thermal process of a Li-ion battery under unknown boundary heat exchange.

For the sake of paper length, some further discussions are referred to the supplementary file.

VI. CONCLUSIONS

Modeling of the thermal process of a Li-ion battery is of significance. To this end, this paper proposes a spatial correlation based incremental learning for spatiotemporal modeling. The proposed method is KL based and includes three phases. In phase one, a spatial correlation based incremental KL is designed to update the DSBFs of the nominal model efficiently. By using a forgetting factor in the incremental KL, the recent spatiotemporal dynamics can be captured effectively. In phase two, an RBFNN based temporal model is constructed for prediction. Finally, by time/space synthesis, the temperature distribution can be estimated. Simulations and experiments verify that:

- The proposed method shows better or at least competitive performance against other methods.
- The proposed method can be applied to a single battery cell as well as a composite cell successfully.

In fact, the proposed model is a group of ODEs, which is simpler than the original PDE. However, it still could be a bit complex for control design as the control design usually requires linear models. Further simplification is needed for real control application.

Of course, as a data-driven method, some sensors are needed for data acquisition. Note that the aim of this paper is to enhance the conventional data-driven methods to model thermal processes with unknown boundary heat exchange. The reduction of sensors would be considered in the future work as summarized in Remark 2 and Remark 3.

In addition, since the proposed method is effective for a single battery cell as well as a composite cell, it would be interesting to apply it to a battery pack and a BMS. This topic can also be considered as the future work and the potential techniques are clarified in Remark 1.

REFERENCES

[1] L. Lu, X. Han, J. Li, J. Hua, and M. Ouyang, "A review on the key issues for lithium-ion battery management in electric vehicles," *J. Power Sources*, vol. 226, pp. 272–288, 2013.

[2] T. M. Bandhauer, S. Garimella, and T. F. Fuller, "A critical review of thermal issues in lithium-ion batteries," *J. Electrochem. Soc.*, vol. 158, no. 3, pp. R1–R25, 2011.

[3] Z. Liu and H.-X. Li, "A spatiotemporal estimation method for temperature distribution in lithium-ion batteries," *IEEE T. Ind. Inform.*, vol. 10, no. 4, pp. 2300–2307, 2014.

[4] Y. Feng and H.-X. Li, "Detection and spatial identification of fault for parabolic distributed parameter systems," *IEEE T. Ind. Electron.*, 2018, DOI: 10.1109/TIE.2018.2877188.

[5] K. K. Xu, H.-X. Li, and H. D. Yang, "Local properties embedding based nonlinear spatiotemporal modeling for lithium-ion battery thermal process," *IEEE T. Ind. Electron.*, vol. 65, no. 12, pp. 9767–9776, 2018.

[6] S. Abada, G. Marlair, A. Lecocq, M. Petit, V. Sauvant-Moynot, and F. Huet, "Safety focused modeling of lithium-ion batteries: A review," *J. Power Sources*, vol. 306, pp. 178–192, 2016.

[7] X. Lin, H. Perez, S. Mohan, J. B. Siegel, A. G. Stefanopoulou, Y. Ding, and M. P. Castanier, "A lumped-parameter electro-thermal model for cylindrical batteries," *J. Power Sources*, vol. 257, pp. 1–11, 2014.

[8] K. S. Hariharan, "A coupled nonlinear equivalent circuit–thermal model for lithium ion cells," *J. Power Sources*, vol. 227, pp. 171–176, 2013.

[9] M. Doyle, T. F. Fuller, and J. Newman, "Modeling of galvanostatic charge and discharge of the lithium/polymer/insertion cell," *J. Electrochem. Soc.*, vol. 140, no. 6, pp. 1526–1533, 1993.

[10] A. M. Bizeray, S. Zhao, S. R. Duncan, and D. A. Howey, "Lithium-ion battery thermal-electrochemical model-based state estimation using orthogonal collocation and a modified extended kalman filter," *J. Power Sources*, vol. 296, pp. 400–412, 2015.

[11] Y. Feng and H.-X. Li, "Dynamic spatial independent component analysis based abnormality localization for distributed parameter systems," *IEEE T. Ind. Inform.*, 2019, DOI:10.1109/TII.2019.2900226.

[12] Z. Wang, H.-X. Li, and C. Chen, "Reinforcement learning based optimal sensor placement for spatiotemporal modeling," *IEEE T. Cyber.*, 2019, DOI: 10.1109/TCYB.2019.2901897.

[13] U. Kim, C. Shin, and C. Kim, "Modeling for the scale-up of a lithium-ion polymer battery," *J. Power Sources*, vol. 189, pp. 841–846, 2009.

[14] M. Guo and R. E. White, "A distributed thermal model for a li-ion electrode plate pair," *J. Power Sources*, vol. 221, pp. 334–344, 2013.

[15] P. W. Northrop, *Multiscale Modeling, Reformulation, and Efficient Simulation of Lithium-Ion Batteries*. Washington University in St. Louis, 2014.

[16] P. W. Northrop, V. Ramadesigan, S. De, and V. R. Subramanian, "Coordinate transformation, orthogonal collocation, model reformulation and simulation of electrochemical-thermal behavior of lithium-ion battery stacks," *J. Electrochem. Soc.*, vol. 158, no. 12, pp. A1461–A1477, 2011.

[17] P. W. Northrop, M. Pathak, D. Rife, S. De, S. Santhanagopalan, and V. R. Subramanian, "Efficient simulation and model reformulation of two-dimensional electrochemical thermal behavior of lithium-ion batteries," *J. Electrochem. Soc.*, vol. 162, no. 6, pp. A940–A951, 2015.

[18] P. Tagade, K. Hariharan, S. M. Kolake, T. Song, and D. Oh, "Stochastic spectral projection of electrochemical thermal model for lithium-ion cell state estimation," *J. Power Sources*, vol. 343, pp. 520–535, 2017.

[19] H. Park and D. Cho, "The use of the karhunen-loeve decomposition for the modeling of distributed parameter systems," *Chem. Eng. Sci.*, vol. 51, no. 1, pp. 81–98, 1996.

[20] L. Cai and R. E. White, "Reduction of model order based on proper orthogonal decomposition for lithium-ion battery simulations," *J. Electrochem. Soc.*, vol. 156, no. 3, pp. A154–A161, 2009.

[21] C. Multiphysics, "v. 5.2," *COMSOL AB, Stockholm, Sweden*, 2015.

[22] Z. Liu and H.-X. Li, "Extreme learning machine based spatiotemporal modeling of lithium-ion battery thermal dynamics," *J. Power Sources*, vol. 277, pp. 228–238, 2015.

[23] Z. Wang and H.-X. Li, "Incremental spatiotemporal learning for online modeling of distributed parameter systems," *IEEE T. Syst. Man. Cy.-S.*, 2018, DOI: 10.1109/TSMC.2018.2810447.

[24] Y. Kim, S. Mohan, J. B. Siegel, A. G. Stefanopoulou, and Y. Ding, "The estimation of temperature distribution in cylindrical battery cells under unknown cooling conditions," *IEEE T. Contr. Syst. T.*, vol. 22, no. 6, pp. 2277–2286, 2014.

[25] M. Wang and H.-X. Li, "Real-time estimation of temperature distribution for cylindrical lithium-ion batteries under boundary cooling," *IEEE T. Ind. Electron.*, vol. 64, no. 3, pp. 2316–2324, 2017.

[26] B.-C. Wang and H.-X. Li, "A sliding window based dynamic spatiotemporal modeling for distributed parameter systems with time-dependent boundary conditions," *IEEE T. Ind. Inform.*, vol. 15, no. 4, pp. 2044–2053, 2019.

[27] J. Park and I. Sandberg, "Universal approximation using radial-basis-function networks," *Neural Computation*, vol. 3, no. 2, pp. 246–257, 1991.

[28] U. S. Kim, J. Yi, C. B. Shin, T. Han, and S. Park, "Modelling the thermal behaviour of a lithium-ion battery during charge," *J. Power Sources*, vol. 196, no. 11, pp. 5115–5121, 2011.

[29] Y. Wang, Z. Cai, and Q. Zhang, "Differential evolution with composite trial vector generation strategies and control parameters," *IEEE T. Evolut. Comput.*, vol. 15, no. 1, pp. 55–66, 2011.

[30] J. Lee, K. Choi, N. Yao, and C. Christianson, "Three-dimensional thermal modeling of electric vehicle batteries," *J. Electrochem. Soc.*, vol. 133, no. 7, pp. 1286–1291, 1986.

[31] M. R. Khan and S. K. Kaer, "Three dimensional thermal modeling of li-ion battery pack based on multiphysics and calorimetric measurement," in *2016 IEEE VPPC*. IEEE, 2016, pp. 1–6.

[32] H. Sun, X. Wang, B. Tossan, and R. Dixon, "Three-dimensional thermal modeling of a lithium-ion battery pack," *J. Power Sources*, vol. 206, pp. 349–356, 2012.

[33] J. Li, L. Zou, F. Tian, X. Dong, Z. Zou, and H. Yang, "Parameter identification of lithium-ion batteries model to predict discharge behaviors using heuristic algorithm," *J. Electrochem. Soc.*, vol. 163, no. 8, pp. 1646–1652, 2016.

[34] A. Jokar, B. Rajabloo, M. Désilets, and M. Lacroix, "An inverse method for estimating the electrochemical parameters of lithium-ion batteries i. methodology," *J. Electrochem. Soc.*, vol. 163, no. 14, pp. A2876–A2886, 2016.

[35] D. R. Jones, M. Schonlau, and W. J. Welch, "Efficient global optimization of expensive black-box functions," *J. Global Optim.*, vol. 13, no. 4, pp. 455–492, 1998.

[36] A. Gupta, Y.-S. Ong, and L. Feng, "Insights on transfer optimization: Because experience is the best teacher," *IEEE T. Emerg. Top. Comput. Intell.*, vol. 2, no. 1, pp. 51–64, 2018.

[37] X.-B. Meng, H.-X. Li, and H.-D. Yang, "Evolutionary design of spatiotemporal leaning model for thermal distribution in lithium-ion batteries," *IEEE T. Ind. Inform.*, 2018, DOI 10.1109/TII.2018.2866468.

Bing-Chuan Wang received the B.E. degree in automation and the M.S. degree in control science and engineering both from Central South University, Changsha, China, in 2013 and 2016, respectively. He is currently pursuing the Ph.D. degree with the City University of Hong Kong, Hong Kong.

His current research interests include system modeling, battery management system, and evolutionary computation.

Han-Xiong Li (S'94-M'97-SM'00-F'11) received his B.E. degree in aerospace engineering from the National University of Defense Technology, China in 1982, M.E. degree in electrical engineering from Delft University of Technology, The Netherlands in 1991, and Ph.D. degree in electrical engineering from the University of Auckland, New Zealand in 1997.

He is a professor in the Department of SEEM, City University of Hong Kong. He has a broad experience in both academia and industry. He has authored 2 books and about 20 patents, and published more than 200 SCI journal papers with h-index 42 (web of science). His current research interests include process modeling and control, system intelligence, distributed parameter systems, and battery management system.

Dr. Li serves as Associate Editor for IEEE Transactions on SMC: System, and was associate editor for IEEE Transactions on Cybernetics (2002-2016) and IEEE Transactions on Industrial Electronics (2009-2015). He was awarded the Distinguished Young Scholar (overseas) by the China National Science Foundation in 2004, a Chang Jiang professorship by the Ministry of Education, China in 2006, and a national professorship in China Thousand Talents Program in 2010. He serves as a distinguished expert for Hunan Government and China Federation of Returned Overseas Chinese. He is a Fellow of the IEEE.

Hai-Dong Yang received his B.E. degree from Jilin University of Technology in 1997, M.E. degree from South China Agricultural University in 2000, and Ph.D. degree from South China University of Technology in 2005.

He is currently a Professor with the School of Electromechanical Engineering, Guangdong University of Technology. He has authored 2 books and 23 patents, and published more than 30 SCI journal papers. His current research interests are in intelligent manufacturing, green manufacturing, and internet of things.